

Late Quaternary sedimentation within a submarine channel–levee system offshore Cap Timiris, Mauritania

C. Zühlsdorff^{*}, K. Wien¹, J.-B.W. Stuut, R. Henrich

University of Bremen, Faculty of Geosciences, Klagenfurter Straße, 28359 Bremen, Germany

Received 11 May 2006; received in revised form 9 February 2007; accepted 16 February 2007

Abstract

Aeolian and fluvial sediment transport to the Atlantic Ocean offshore Mauritania were reconstructed based on grain-size distributions of the carbonate-free silt fraction of three marine sediment records of Cap Timiris Canyon to monitor the climatic evolution of present-day arid north-western Africa. During the late Pleistocene, predominantly coarse-grained particles, which are interpreted as windborne dust, characterise glacial dry climate conditions with a low sea level and extended sand seas that reach onto the exposed continental shelf off Mauritania. Subsequent particle fining and the abrupt decrease in terrigenous supply are attributed to humid climate conditions and dune stabilisation on the adjacent African continent with the onset of the Holocene humid period. Indications for an ancient drainage system, which was discharging fluvial mud offshore via Cap Timiris Canyon, are provided by the finest end member for early to mid Holocene times. However, in comparison to the Senegal and Niger River further south, the river system connecting Cap Timiris Canyon with the Mauritanian hinterland was starved during the late Holocene and is non-discharging under present-day arid climate conditions.

© 2007 Elsevier B.V. All rights reserved.

Keywords: continental margin; north-west Africa; sedimentary processes; Holocene; late Pleistocene; end members; aeolian supply; marine sediments

1. Introduction

Continental margin sedimentation along the north-east Atlantic has been studied in different climatic zones from the glaciated and glacially-influenced European margins to the non-glaciated east Atlantic margin south of 26°N (e.g., Mienert and Weaver, 2003 and references therein) and is influenced by hemipelagic sedimentation as well as

sediment redistribution by along- and down-slope transport processes. These sedimentary processes are governed by Quaternary glacial–interglacial variability and drastic climate changes all along this continental margin. Within the different climatic zones, however, these processes have different impacts on margin sedimentation (Weaver et al., 2000).

Along the non-glaciated north-west African continental margin, sedimentation is characterised by high sedimentation rates due to high marine productivity and the terrigenous, at present predominantly aeolian, sediment supply (e.g., Ratmeyer et al., 1999; deMenocal et al., 2000; Weaver et al., 2000). Furthermore, sediment remobilisation by gravity flows is also important along the

^{*} Corresponding author. Now at: University of Bergen, Department of Earth Science, Allégaten 41, 5007 Bergen, Norway. Tel.: +47 5558 8112.

E-mail address: christine.zuehlsdorff@geo.uib.no (C. Zühlsdorff).

¹ Now at: Fugro-Robertson, Llandudno, North Wales, LL30 1SA, United Kingdom.

north-west African continental margin (e.g., Rust and Wienecke, 1973; Bein and Fütterer, 1977; Sarnthein and Diester-Haass, 1977; Diester-Haass, 1981; Kounkou and Barousseau, 1988; Faugères et al., 1989; Wynn et al., 2000) and sediments derived from the shelf and upper margin are transported downslope into the deep sea. Submarine canyons can act as sediment traps and are considered to be preferred pathways for downslope sediment transport notably by turbidity currents. Previous studies have shown that a number of smaller channels and incised valleys exist along the Mauritanian and Senegalese margins (Jakobi and Hayes, 1982). During *RV Meteor* expedition M58/1 of the Research Center Ocean Margins (RCOM) at the University of Bremen (Schulz and cruise participants, 2003) a large submarine meandering canyon system, which was named the Cap Timiris Canyon, was discovered offshore Mauritania (Krstel et al., 2004). Although the continental margin of north-west Africa between 15°N and 26°N is presently dominated by arid climate conditions in the Sahara Desert and receives no significant fluvial input (Weaver et al., 2000), the origin of Cap Timiris Canyon is assumed, as many other passive margin submarine canyons, to be related to a major sub-aerial river system in the past (Vörösmarty et al., 2000; Antobreh and Krstel, 2006).

This study aims to provide insights into late Quaternary sedimentation along this submarine meandering canyon system off Mauritania. The sediment records presented here have been recovered from the upper as well as from the lower Cap Timiris Canyon, both from levee and inside canyon positions and provide new information about spatial and temporal variations of sedimentary regimes within this submarine canyon system as well as the climatic situation of the adjacent Sahara Desert and its evolution during the past ~70 ka. Principal objectives of this study are (1) to assess hemipelagic sedimentation along and within a submarine meandering canyon system offshore a major present-day desert, and (2) to assess the analogies of pronounced shifts in depositional settings of continental margin sedimentation with climate changes in the African hinterland. Furthermore, indications for more humid phases on the African continent during late Quaternary times also raise the question on the existence and activity of an ancient river system connected with Cap Timiris Canyon.

2. Investigation area

2.1. Margin morphology and oceanography

The southern part of the Mauritanian continental margin up to Cap Timiris is characterised by a narrow

shelf, between 30 and 40 km wide, and moderately steep slope angles of 2.5 to 3° (Antobreh and Krstel, 2006). North of Cap Timiris the shelf broadens significantly represented by the Banc d'Arguin, a shallow marine platform. The continental slope off the Banc d'Arguin is very steep with angles up to about 6° (Antobreh and Krstel, 2006), and especially to the south it is closely incised by numerous canyons. Only a few of these canyons can be traced on to the shelf (e.g., Bein and Fütterer, 1977; Diester-Haass, 1981).

The north-west African continental margin is characterised by the southward-flowing Canary Current and a northward-flowing counter current. Offshore Cape Blanc the interaction of these currents results in a cyclonic eddy circulation and a deflection of the Canary Current from the coast (Bein and Fütterer, 1977). Only a minor part of this flow continues as far south as Cape Verde and becomes the Guinea Current further south. The deeper water masses, characterised by the North Atlantic Deep Water (NADW) and Antarctic Bottom Water (AABW), are thought to be presently fairly weak ($<5 \text{ cm s}^{-1}$), whereas in areas where currents are focussed by morphology or due to additional tidal components, velocities may increase to 20 cm s^{-1} (Lonsdale, 1982; Sarnthein et al., 1982). Presently, no strong currents are suggested to be active within the canyons along this margin, which is indicated by very fine-grained mud blankets found in some of these canyons (Seibold et al., 1976; cited in Bein and Fütterer, 1977), although seafloor topography may influence sedimentation processes locally.

2.2. Sedimentation, climate conditions and sediment transport

Coastal upwelling usually favours high marine productivity. Generally, upwelling off north-west Africa is concentrated on the outer shelf and shelf edge in a band of about 50 km width, although filaments of cold, nutrient-rich upwelling waters occasionally reach several hundreds kilometres offshore (Van Camp et al., 1991). In the Banc d'Arguin region upwelling has also been observed in the head of some canyons (Shaffer, 1976). High concentrations of organic-rich sediments are only observed locally in narrow belts along the north-west African continental margin (i.e., the shelf area off Cape Blanc, which is after Fütterer (1983) the most productive upwelling area). Most of the middle and outer shelf between ~29°N and ~21°N is covered with carbonate sand, muddy sediments with less than 75% carbonate content occur only in patches on the innermost shelf and at water depths exceeding 500 m on the continental slope (McMaster and Lachance, 1969; Summerhayes, 1983). In contrast, in coastal upwelling

areas off Senegal and Mauritania biological productivity is reduced (Hagen, 2001), and south of Cape Blanc carbonate sands dominate only in some places (McMaster and Lachance, 1969). The terrigenous sedimentation off Mauritania is presently affected by prevailing arid climate conditions in the adjacent Sahara Desert. Climate conditions in north-west Africa changed significantly during late Quaternary times comprising arid and humid phases (e.g., Koopmann, 1981; Sarnthein et al., 1982; Dupont et al., 1989; Lézine and Casanova, 1989; Stabell, 1989; Tiedemann et al., 1989). Extensive sand seas and large dune fields were generated during late Pleistocene and Holocene times (Lancaster et al., 2002), suggesting a strong impact on terrigenous sedimentation processes off north-west Africa. At present, terrigenous sediment supply off Mauritania is dominated by aeolian dust, while fluvial discharge is mainly restricted to the Moroccan and Senegalese margins (e.g., Koopmann, 1981; Hillier, 1995; Rattmeyer et al., 1999; Holz et al., 2004). During the climatic optimum around 6 ka before present indications for more humid conditions and a reduced extension of the arid environment, compared to the present, as well as enhanced fluvial discharge of the Senegal River are indicated by various studies (e.g., Sarnthein, 1978; Koopmann, 1981). More recently, paleohydrological data indicate several periods with higher rainfall than present in the Sahelian as well as in the Saharan climatic zones from 9 to 7 ka BP and from 4 to 2.5 ka BP (Lézine and Casanova, 1989). Based on east Saharan studies, the Holocene African Humid Period spans the interval between 9 and 6 ka BP (Ritchie et al., 1985; Roberts, 1998; Kuper and Kröpelin, 2006). For this time span, many studies reveal a phase of maximum humidity also in North Africa, which is evidenced by overall wet savannah landscape with numerous small and large lakes (e.g., Gasse, 2000 and references therein). At the southern margin of the Sahara between 19°N and 22°N the desertic steppes vegetation was replaced by a typical Sudano-Sahelian pseudo-steppes around 9 ka BP (Lézine, 1987; Lézine and Casanova, 1989). The duration of this northward extension varied with latitude. In western Mauritania, the early Holocene phytogeographic pattern remained unchanged until ca. 6.3 ka BP (Lézine and Casanova, 1989). However, humid conditions in western Africa are assumed to have initially commenced around 14.5–11.5 ka BP (Lézine and Casanova, 1989, and references therein; deMenocal et al., 2000) and thus before the Holocene African Humid Period (Ritchie et al., 1985; Roberts, 1998), following the glacial hyperarid climate during the latest Pleistocene (e.g., Sarnthein, 1978; Koopmann, 1981; Street-Perrott and Perrott, 1990; Gasse and Van Campo, 1994).

Beside the dominantly pelagic and hemipelagic sedimentation, i.e., settling of dead planktonic organisms or terrigenous particles accomplished by large dust plumes, the spectrum of sedimentary regimes off Mauritania also includes sediment redistribution processes such as along-slope transport by bottom currents, and downslope, gravity-driven processes involving mass wasting (e.g., Bein and Fütterer, 1977; Jakobi and Hayes, 1982; Krastel et al., 2004; Krastel et al., 2006; Wien et al., 2006).

2.3. Cap Timiris Canyon

Cap Timiris Canyon incises the passive continental margin off northern Mauritania, slightly north of Cap Timiris (Fig. 1). Its tributary system has been eroded into the continental shelf and upper slope and acts as a natural sediment trap. Cap Timiris Canyon was investigated by combined techniques of seismic and hydroacoustic, geochemical and sedimentological approaches (Schulz and cruise participants, 2003). It was mapped for a total length of ~290 km along its meandering channel axis from the shelf edge at water depths of ~50 m down to about 3050 m (Antobreh and Krastel, 2006). However, in the General Bathymetric Chart of the Oceans (GEBCO, 2003) it becomes obvious that this system continues its pathway for hundreds of kilometres beyond the mapped track into the deep sea. Cap Timiris Canyon is predominantly V-shaped and shows fluvial features including tributaries and meander patterns, cut-off loops and terraces. Due to a different character and two distinct trends, Cap Timiris Canyon can be divided into an upper NE–SW orientated part and lower part with a predominantly E–W direction (Antobreh and Krastel, 2006).

The origin of Cap Timiris Canyon is ascribed to an ancient river system in the adjacent presently arid Sahara Desert that breached the shelf during Plio/Pleistocene times (Antobreh and Krastel, 2006). During the phase of canyon development it is assumed that turbidity currents incised the seafloor by transporting huge amounts of shelf and upper margin sediments to the deep sea. During the Holocene however, turbidite activity of the system changed. Small-scale turbidity currents occurred, which delivered very fine-grained sediments with less potential for erosion and which furthermore, were confined to the canyon and did not overspill onto the levees.

3. Materials and methods

This study focuses on three gravity cores, GeoB 8502–2, GeoB 8507–3 and GeoB 8509–2 (Fig. 1), which were recovered from the Cap Timiris Canyon system offshore Mauritania during *R/V Meteor* cruise

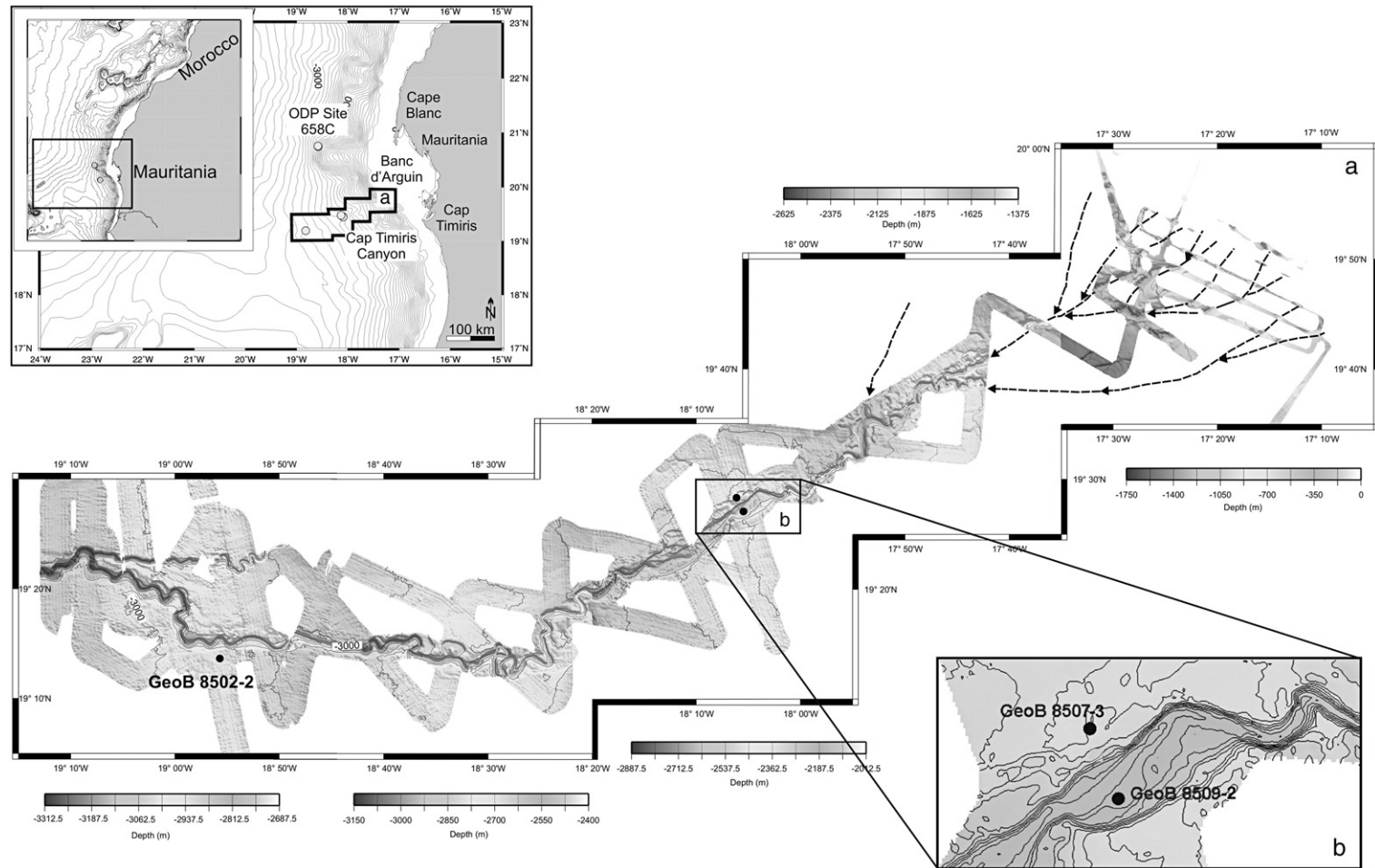


Fig. 1. Map of the investigation area off Cap Timiris, Mauritania. The detailed bathymetric map of the Cap Timiris Canyon is a black and white version of the colour map published by Krastel et al. (2004). It is plotted from Hydrosweep data of *RV Meteor* cruise M58/1 (Schulz and cruise participants, 2003) and indicates the investigated core positions along this meandering system offshore Saharan Africa. Seismic images indicate horizontal layers and depositional rather than erosional features at this location for the recent past, although tectonic activity has surely been relevant during the early evolution of Cap Timiris Canyon (Antobreh and Krastel, 2006). This is also supported by the investigated sediment deposits. Despite interbedded turbidites, the sediment cores do not indicate significant omission of hemipelagic material (Wien et al., 2006).

M58/1 in April/May 2003 (Schulz and cruise participants, 2003). Cores GeoB 8502–2 (19°13.27' N, 18°56.04' W; 2956 m water depth; 14,8 m long) and GeoB 8507–3 (19°28.50' N, 18°05.97' W; 2411 m water depth; 10 m long) were retrieved from levee structures of the lower and upper Cap Timiris Canyon. In addition, the 9 m long sediment core GeoB 8509–2 (19°27.03' N, 18°05.34' W; 2585 m water depth) was recovered from inside the canyon system, where the canyon widens significantly, building the first of two basins of 7.5 km width (Antobreh and Krastel, 2006).

3.1. Age models

Age constraints for the sediment cores are provided by downcore Ca content profiles of the hemipelagic sequences, which were correlated to variations in the carbonate content of oxygen isotope and radiocarbon dated reference cores, CD53–30 (Matthewson et al., 1995), GeoB 7919–5 (Wien et al., 2006), and ODP 658C (deMenocal et al., 2000) off Mauritania, respectively. According to the core-to-core correlation of Ca contents of intra-canyon core GeoB 8509–2 with the carbonate content of ODP site 658C off Cape Blanc, sediment record GeoB 8509–2 dates back to ~15 ka (Wien et al., 2006). In addition, the age model of this intra-canyon core is considerably improved by ten accelerator mass spectrometer radiocarbon (AMS ^{14}C) dates on monospecific samples of the planktonic foraminifer *Globigerinoides ruber* measured at the Leibniz Labor, Kiel University (Table 1). Related to the radiocarbon dates and linear interpolation between the dates, the sediment record from the canyon covers the past 13 ka and thus illustrates an offset to the core-to-core correlation. This

offset should be kept in mind for the correlation of the three sediment cores and the discussion. Radiocarbon ages were calibrated using CALIB 5.0.1 (Stuiver and Reimer, 1993) and the marine04.14c dataset (Hughen et al., 2004) assuming a conservative reservoir age of 500 ± 50 years due to an upwelling of older subsurface waters in this region (deMenocal et al., 2000). Calibrated ages were rounded to the nearest decade (Stuiver and Reimer, 1993) and are reported as cal. ka BP.

3.2. Sediment structures

The investigated sediment cores of the Cap Timiris Canyon system are characterised by autochthonous hemipelagic deposits, which are intercalated by turbidites. A careful distinction between hemipelagic and gravity-driven sediments is necessary in order to correctly interpret the sedimentological and geochemical data as well as to establish a meaningful stratigraphic concept. Mostly, turbidite sequences were easily discerned by visual examination of the sediment cores. Additionally, X-ray radiographs were made of 1-cm thick sediment slices with 10×25 cm dimensions to improve the visualisation of internal structures especially for the finer sediment sequences, where turbidites were difficult to identify visually only. Thus, visual investigations of the sediments are here combined with corresponding X-ray radiographs to differentiate between hemipelagic sedimentation and mass-transport deposits with 0.5 cm accuracy. The top sections of turbidite deposits are frequently obscured by intense bioturbation and therefore it was often difficult to distinguish them from the overlying, fine-grained hemipelagic muds. In these cases, the transition of turbiditic into hemipelagic

Table 1
AMS radiocarbon dates on ten monospecific samples of planktonic foraminifer *Globigerinoides ruber* of gravity core GeoB 8509–2

Sample depth (cm)	Corrected sample depth (cm)	^{14}C age (yr BP)	Cal. age BP	1 σ cal. age BP (relative area)	\pm Error	$\delta^{13}\text{C}$ (‰)
5	5	650 \pm 25	160	145–168 (0.26)	25	0.15 \pm 0.22
			210	173–244 (0.74)	40	
35	10	1060 \pm 40	550	516–585 (0.74)	35	0.69 \pm 0.22
			590	575–597 (0.26)	15	
110	44	2085 \pm 40	1550	1491–1605 (1.0)	60	-0.14 \pm 0.25
155	64.5	2795 \pm 50	2390	2323–2457 (1.0)	70	2.37 \pm 0.32
215	124.5	4345 \pm 35	4350	4297–4406 (1.0)	60	-2.80 \pm 0.25
305	193.5	7595 \pm 45	7960	7913–8003 (1.0)	40	-2.98 \pm 0.37
460	262.5	9385 \pm 55	10,040	10,040–10,048 (0.03)	5	-3.18 \pm 0.19
			10,140	10,070–10,209 (0.97)	70	
515	317.5	9980 \pm 55	10,780	10,658–10,905 (1.0)	125	-2.93 \pm 0.24
720	375	10,860 \pm 50	12,200	12,083–12,305 (1.0)	115	-1.13 \pm 0.29
881	454.5	11,350 \pm 70	12,850	12,816–12,880 (1.0)	30	-0.49 \pm 0.28

^{14}C ages were calibrated using CALIB 5.0.1 (Stuiver and Reimer, 1993) and the marine 04.14c dataset (Hughen et al., 2004) assuming a conservative reservoir age of 500 ± 50 years due to the upwelling regime.

sediments was defined by the significant increase of foraminifers, since turbidite mud is supposed to contain less foraminifer brought in through bioturbation.

3.3. Carbonate content

Downcore total carbon (C_{tot}) and organic carbon (C_{org}) contents were determined for all bulk samples of the three cores using a Leco CS-300 elemental analyser. Organic and total carbon values were measured in homogenised sub-samples. For the determination of organic carbon, carbonate was removed by adding repeatedly hydrochloric acid (12.5% HCl). The calcium carbonate content was finally calculated by the deviation of total carbon (C_{tot}) and organic carbon (C_{org}) using the following equation: $[\text{CaCO}_3 = (C_{\text{tot}} - C_{\text{org}}) * 8.33]$.

3.4. Grain sizes and end-member modelling of the hemipelagic sediments

For grain-size analysis, all hemipelagic samples were prepared as follows: samples were freeze-dried and, after removing the organic matter through oxidation with hydrogen-peroxide (10% H_2O_2), the sand ($>63 \mu\text{m}$) was separated from the fine fraction ($<63 \mu\text{m}$) by wet-sieving. Afterwards, clay particles ($<2 \mu\text{m}$) were extracted from the silt fraction ($63\text{--}2 \mu\text{m}$) by a repeated settling procedure based on Stokes' law, using Atterberg settling tubes. Each fraction was dried and weight percentages were determined. Detailed grain-size spectra were measured for the silt fraction of the hemipelagic sediments with a Micromeritics SediGraph 5100. The principle of this fine-particle size analyser is based on

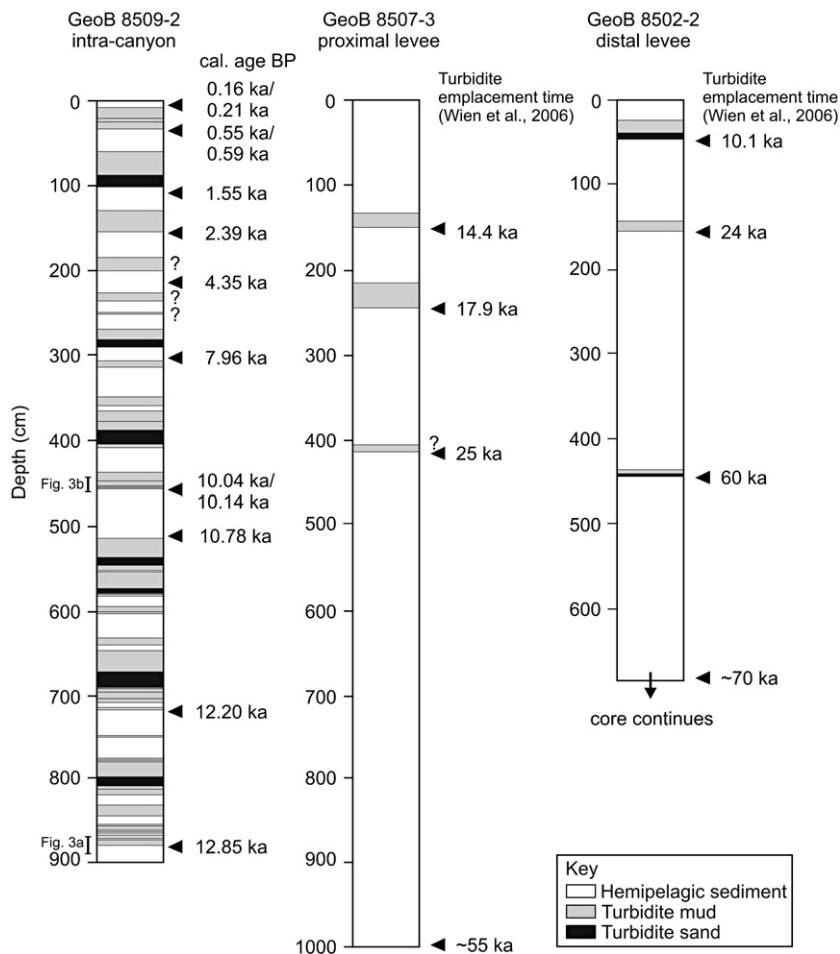


Fig. 2. Interpretive core logs of the sediments recovered from Cap Timiris Canyon indicating hemipelagic deposits and turbiditic sequences. Sediments from the canyon (GeoB 8509–2) are heavily intercalated with thin turbidite deposits of 2 to 40 cm thickness, whereas the levee sediments (GeoB 8502–2 and GeoB 8507–3) are less influenced by turbidity currents. Question marks indicate reworked turbidite deposits. Age control for GeoB 8509–2 is shown by radiocarbon dates. Sediments of GeoB 8507–3 and the investigated upper sequence of GeoB 8502–2 from the proximal and distal levee are correlated to isotope-dated reference cores (Wien et al., 2006) and date back to 55 and ~70 ka, respectively.

sediment settling, thus close to the sediment dynamics in the ocean. In a first run, grain-size spectra between 62.5 and $\sim 2 \mu\text{m}$ (4 and 9 phi) were determined for each bulk silt sample. For the determination of the carbonate-free silt grain-size distribution, samples were recovered after the first run, dried and weighed. The carbonate of the silt fraction was then dissolved with hydrochloric acid (1 N HCl) and washed repeatedly until neutral pH. Drying and weighing of the samples subsequent to carbonate dissolution provided the carbonate content for each silt sample. In a second run, grain-size distributions of the carbonate-free silt fraction were determined according to the analysis of the bulk silt fraction, while the deviation of the carbonate-free from the bulk grain-size distributions offers grain-size spectra of the carbonate silt fraction. Koopmann (1981) showed that silt-sized biogenic silica offshore north-west Africa accounts generally for less than 2% of the total insoluble sediment proportion. Only in the proximal productive upwelling waters and offshore river mouths, the biogenic silica proportion exceeds 2%. Furthermore, grain-size analysis of these sediments indicates that the biogenic silica is relatively uniformly distributed within the size spectrum (Koopmann, 1981). Thus, grain-size distributions of the carbonate-free silt fraction are considered here as the clastic or terrigenous silt fraction.

The supply of terrigenous sediments to the ocean often results from an interaction of various sedimentation processes, which may result in polymodal grain-size distributions. Consequently, measured grain-size

distributions are often difficult to interpret as aeolian dust or fluvial mud supply. As was shown in various studies (Prins and Weltje, 1999; Stuu et al., 2002; Arz et al., 2003; Frenz et al., 2003; Holz et al., 2004; Stuu and Lamy, 2004) grain-size subpopulations can successfully be recognised in polymodal grain-size distributions of marine sediments and be related to sediment transport processes using the end-member modelling approach after Weltje (1994, 1997). This numerical–statistical algorithm aims to explain the variance in the total data set with discrete subpopulations, so-called end members. Goodness-of-fit statistics provide the estimation of the minimum number of end members by calculating the coefficient of determination (r^2), which is required for a satisfactory approximation of the data. r^2 represents the proportion of the variance of each grain-size class that can be reproduced by the approximated data. This proportion is equal to the squared correlation coefficient of the input variables and their approximated values (Weltje, 1997; Prins and Weltje, 1999). In contrast to other non-parametric decomposing approaches like principle component analysis or factor analysis, Weltje's end-member model was designed to deal with 'real' compositions, i.e., the only prescriptions made to the outcome are non-negativity and constant-sum constraints. Hence, the end members are physically meaningful compositions, for instance real grain-size distributions, whereas principle components or factors can have negative values without any physically meaning (Prins and Weltje, 1999; Weltje and Prins, 2003). For

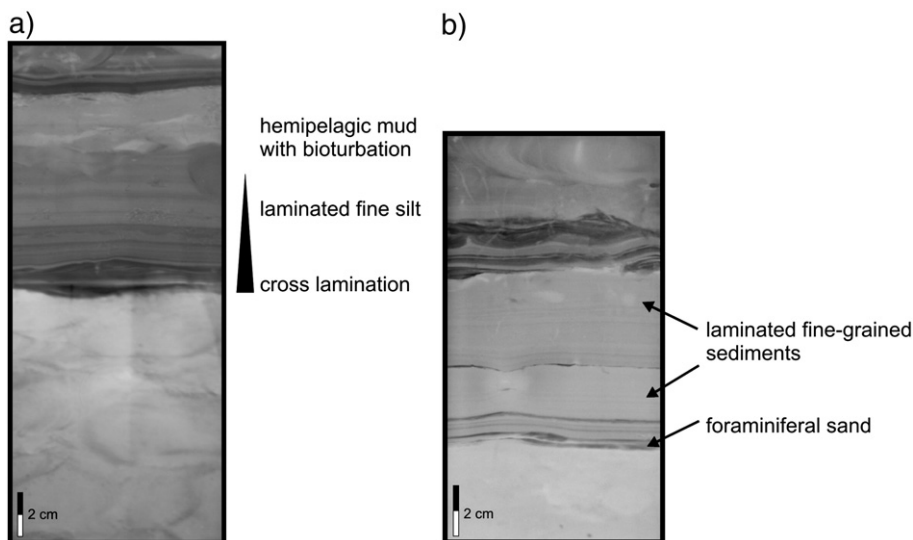


Fig. 3. Photos of the X-ray radiographs of sediment core GeoB 8509–2 showing bioturbated hemipelagic sediments in the lower and upper most part of both pictures as well as turbidite deposits in the middle. Picture a) of 869–890.5 cm core depth shows a fining upward turbidite sequence with cross lamination at the base followed by fine laminated silt and fine-grained hemipelagic mud. Picture b) of 444–462 cm core depth (see Fig. 2) displays very fine-grained laminated mud deposits.

more details on the end-member modelling approach see Weltje (1997), Prins and Weltje (1999) and Weltje and Prins (2003).

4. Results

4.1. Sediment structures

Hemipelagites and turbidites were distinguished based on visual core descriptions and X-ray radiographs. The levee sediments in cores GeoB 8502–2 and GeoB 8507–3 are predominantly hemipelagic deposits and only a few, rather fine-grained, overspill turbidites were identified within these cores. The intra-canyon site GeoB 8509–2 in contrast, is strongly influenced by small-scale turbidity currents and almost half of the core consists of thin (2–40 cm thick) turbidite deposits (Fig. 2). According to the X-ray images of core GeoB 8509–2 two different types of turbidites can be distinguished: i)

fining-upward turbidite sequences (Fig. 3a), and ii) very fine deposits of the upper fine-grained mud suspension (Fig. 3b), here described as mud-turbidites. Additionally, some of these mud-turbidites show a thin layer of foraminifers at the base of the mud-unit. A change from siliciclastic fining-upward turbidites to fine-grained mud turbidites can be observed around 11 ka, while fining-upward turbidite deposits are again observed in the late Holocene.

4.2. Sedimentological and geochemical data

During Pleistocene times between 55 and 48 ka contents of the sand, silt, and clay fractions at both levee sites fluctuate significantly (Fig. 4a–c). Then until the Holocene, 7 to 10 wt.% sand is generally observed in sediments of the proximal levee site of the upper Cap Timiris Canyon, while the silt fraction varies closely around 50 wt.% and the clay fraction is represented with

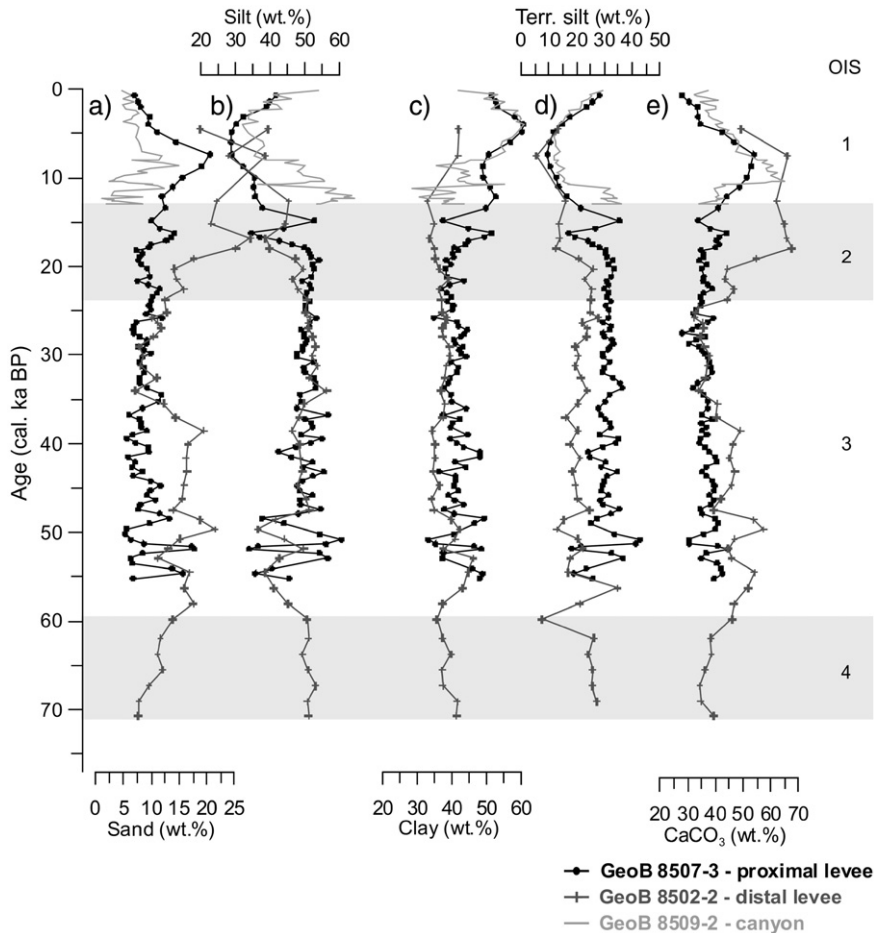


Fig. 4. Sediment texture with weight-percentages for a) sand, b) silt and c) clay fractions, d) terrigenous silt fraction and e) bulk carbonate content of the three gravity cores recovered from Cap Timiris Canyon (see text for details).

40 wt.%. During this time interval, the distal site (GeoB 8502–2) generally displays higher sand but lower clay contents and, compared to the proximal site GeoB 8507–3, almost identical values of about 50 wt.% for the silt fraction. The terrigenous silt fraction (Fig. 4d) shows a very similar trend to the bulk silt fraction, whereas the carbonate (CaCO_3) content follows the trend of the sand fraction (Fig. 4a, e). Throughout the Pleistocene the CaCO_3 content of the proximal levee site ranges between 30 and 35 wt.%. The CaCO_3 contents of the distal levee sediments of core GeoB 8502–2 are however generally enhanced compared to the proximal site. In addition, CaCO_3 contents of this site range from 33 to 70 wt.% and are more variable during isotopic stages 2 and 1.

During the early Holocene, sediments of all three cores are characterised by an increase of the sand fraction, while the silt fraction is extremely reduced. At least in the proximal upper canyon system (sites GeoB 8507–3 and GeoB 8509–2) the clay fraction represents the dominant size class with contents up to 60 wt.%

during the mid to late Holocene. The terrigenous silt fraction significantly decreases with the beginning of the Holocene, whereas contemporaneously the carbonate content of the bulk sediment is increasing (Fig. 4d–e).

Furthermore, Fig. 4 indicates that hemipelagic sedimentation is not only varying temporarily during the past 55 ka, but it is also variable for the three core sites of Cap Timiris Canyon. A comparison of the distal and the more proximal levee sites only indicates that the sand fraction is particularly increased at the distal levee site GeoB 8502–2. The situation is opposite for the clay fraction. Clay contents in sediments of the proximal levee site exceed those in the distal sediments, whereas the silt fraction is relatively balanced between the proximal and distal positions. Including the canyon sediments to the comparison, the parameters of all sites show a similar trend, although absolute contents are reduced or enhanced further offshore. In addition, sand contents are generally higher in the levee sediments than in the canyon deposits.

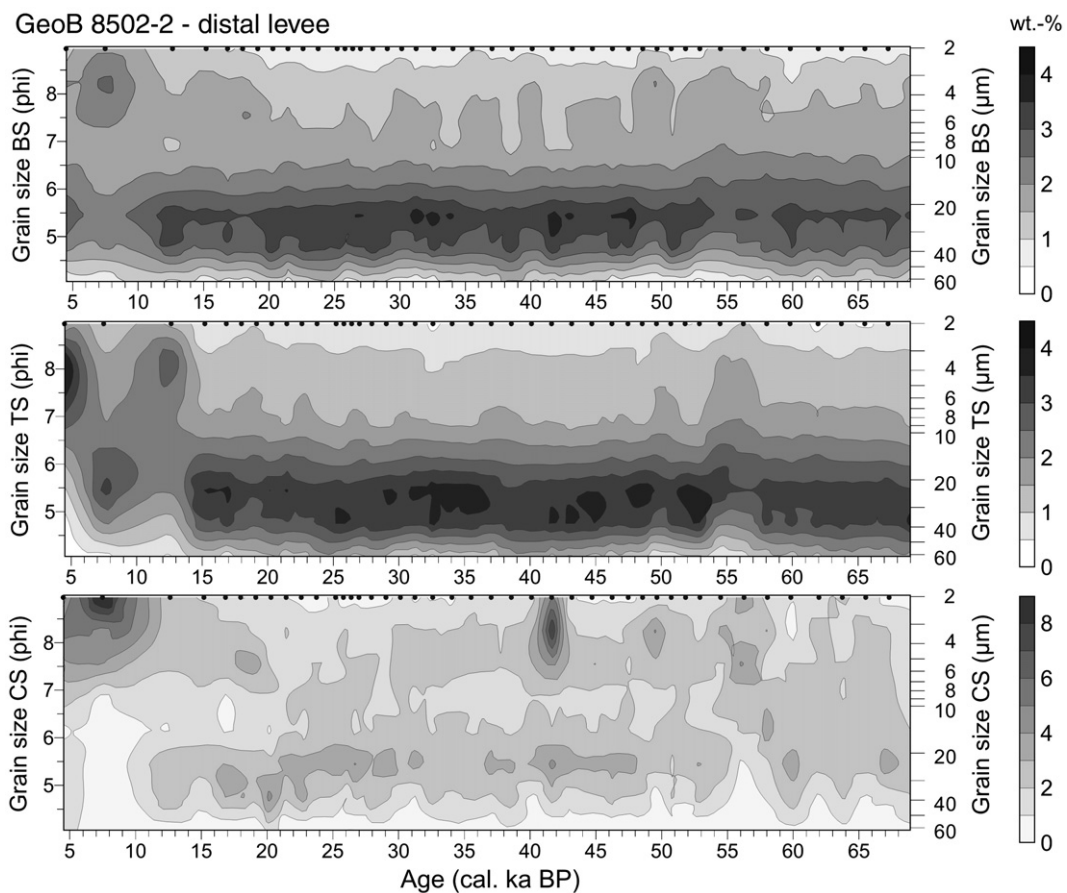


Fig. 5. Grain-size distributions for sediment core GeoB 8502–2 at the distal levee of Cap Timiris Canyon. Displayed are grain sizes for the bulk silt fraction (BS), the terrigenous (TS) and the carbonate silt fraction (CS), respectively, during the past 70 ka.

4.3. Silt grain-size analysis and end-member modelling

Grain-size analysis of the bulk, carbonate-free, and carbonate silt fractions are shown for all hemipelagic sediments of each core (Figs. 5–7). Although the sediment cores from the levees provide a much longer record than the intra-canyon core, a characteristic decrease in grain size can be seen in all considered silt fractions (bulk, carbonate-free = terrigenous, carbonate), and in all three cores around the Pleistocene–Holocene transition.

During the Pleistocene interval until approximately 13 to 11 ka, grain-size distributions of the bulk silt fraction in the levee sediments are generally predominated by coarse silt particles around 22 μm (5.5 phi). Grain sizes of the terrigenous silt fraction are slightly coarser with ~ 25 and 31 μm (5.3 and 5.0 phi) on average, whereas particles of the carbonate fraction are with 11 to 16 μm (6.5 to 6.0 phi) finer than those of the bulk silt fraction during this late Pleistocene interval (Fig. 6). The carbonate silt fraction of

the distal levee (GeoB 8502–2) however, is characterised by bimodal grain-size distributions with modes around $\sim 22 \mu\text{m}$ and 4–5.5 μm (5.5 and 8.0–7.5 phi) during the Pleistocene (Fig. 5).

Around 13 to 11 ka, a transition to overall finer grain sizes occurs for the bulk silt fraction (Figs. 5 and 6). The significant shift to finer modal grain sizes within the bulk silt fraction at the beginning of the Holocene can also be observed for the terrigenous and the carbonate silt fraction of the two levee sites. Beside this shift to finer grain sizes, the carbonate silt fraction shows a bimodal grain-size distribution and additionally contains coarser particles around ~ 22 –31 μm (5.5–5.0 phi).

Comparing grain-size distributions of the neighbouring cores GeoB 8507–3 and GeoB 8509–2 of the upper Cap Timiris Canyon, a fining in particle size and a shift to rather bi- or polymodal grain-size distributions is visible for the bulk silt fraction during early to the middle Holocene (Figs. 6 and 7). This significant change can be

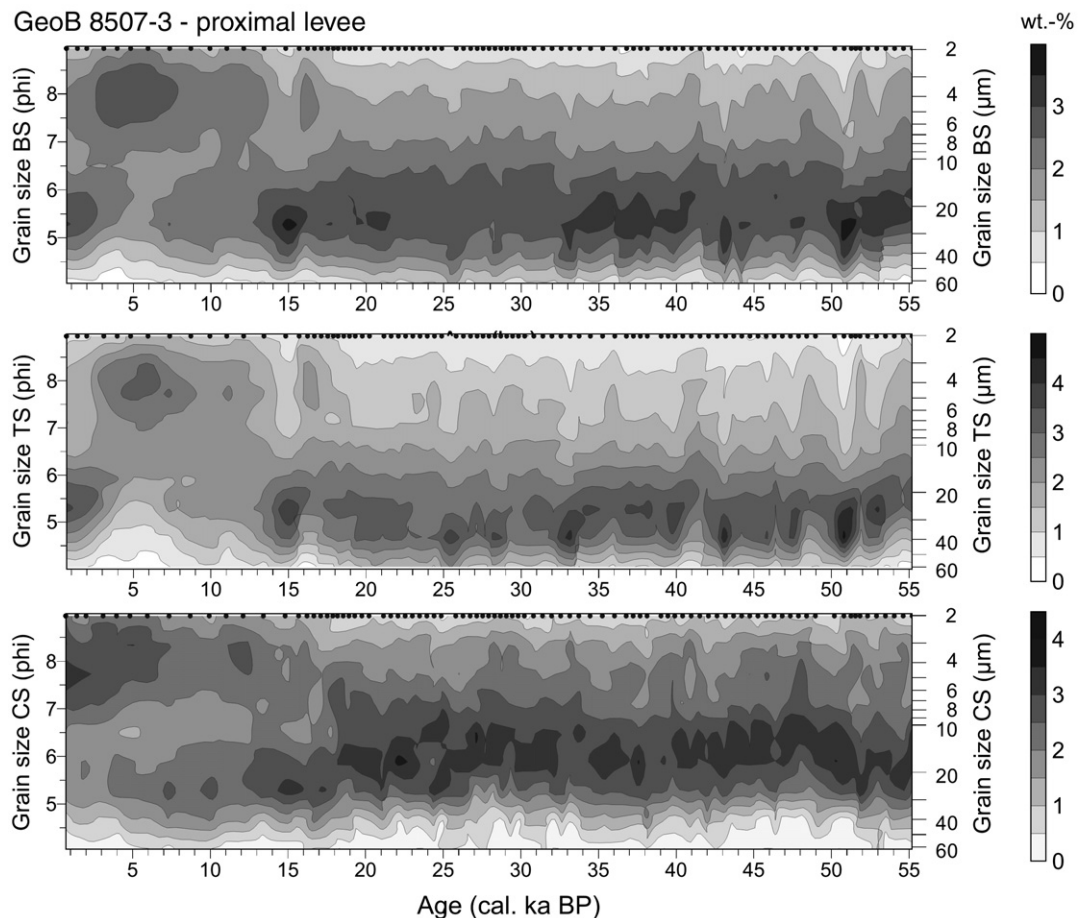


Fig. 6. Grain-size distributions for the past 55 ka of GeoB 8507–3 recovered from the proximal levee of Cap Timiris Canyon. Grain sizes are displayed for the bulk silt (BS), the terrigenous silt (TS) and the carbonate silt fraction (CS), respectively.

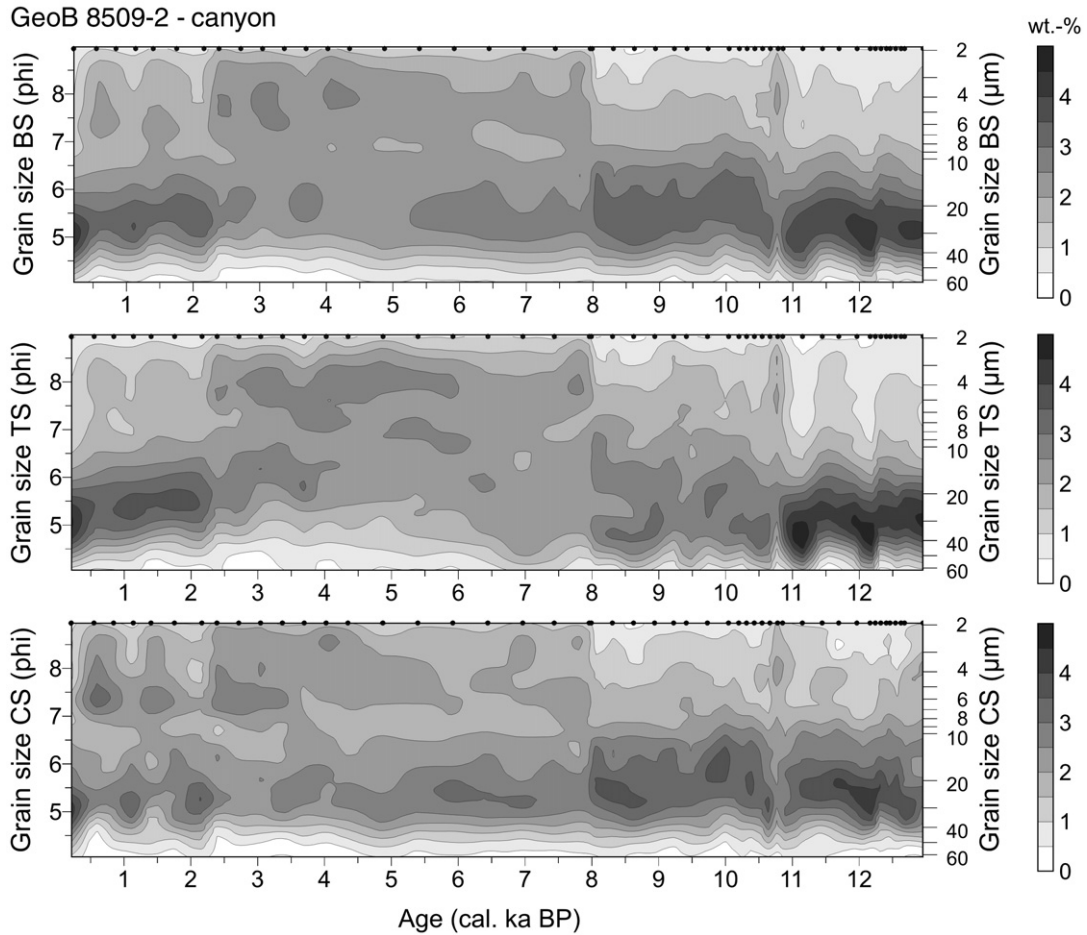


Fig. 7. Grain-size distributions for the intra-canyon core GeoB 8509–2 since the deglacial. Note the different scale. Grain sizes are also shown for the bulk silt (BS), the terrigenous silt (TS) and the carbonate silt fraction (CS), respectively.

identified for the terrigenous and carbonate silt fraction as well, although the dominant modal grain size changes only for the terrigenous fraction from coarse to fine. Thus, coarse particles of the bulk silt fraction are related to coarse silt particles of the carbonate fraction. During the late Holocene, the proximal records (GeoB 8507–3 and GeoB 8509–2) illustrate a shift again to coarser sizes, but only for the terrigenous fraction. The carbonate silt fraction however is characterised by a coarse and fine modal grain size, which were already predominant during the mid Holocene (Figs. 6 and 7).

Sediments usually consist of a mixture of particles that are supplied by different transport processes and are therefore often characterised by polymodal grain-size distributions, which makes it difficult to interpret them in terms of transport processes and sediment origin. The end-member approach after Weltje (1997) was applied to ‘unmix’ distinct grain-size fractions from the data set of all measured grain-size distributions ($N=193$). This

numerical–statistical algorithm aims to explain the variance in the data set with discrete subpopulations, so-called end-member grain-size distributions. The goodness-of-fit statistics of the three records are displayed in Fig. 8. For different end-member solutions ranging from two to ten end members, the coefficient of determination (r^2) per size class is shown versus grain size (Fig. 8a). Additionally, the mean coefficients of determination (r_{mean}^2) are plotted for each of these end-member models (Fig. 8b). The two-end-member model shows low coefficients of determination (<0.6) for a broad size spectrum between 10 and 25 μm . Within the three-end-member model ($r_{\text{mean}}^2=0.81$) the range of only poorly represented grain sizes is reduced to sizes between 10 and 18 μm . A better statistical fit with $r_{\text{mean}}^2=0.91$ is found in the four-end-member model. The finest end member of the three-end-member solution (EM 3; Fig. 8c) shows a modal grain size of $\sim 4 \mu\text{m}$. However, a second coarser mode can be assumed from the grain size

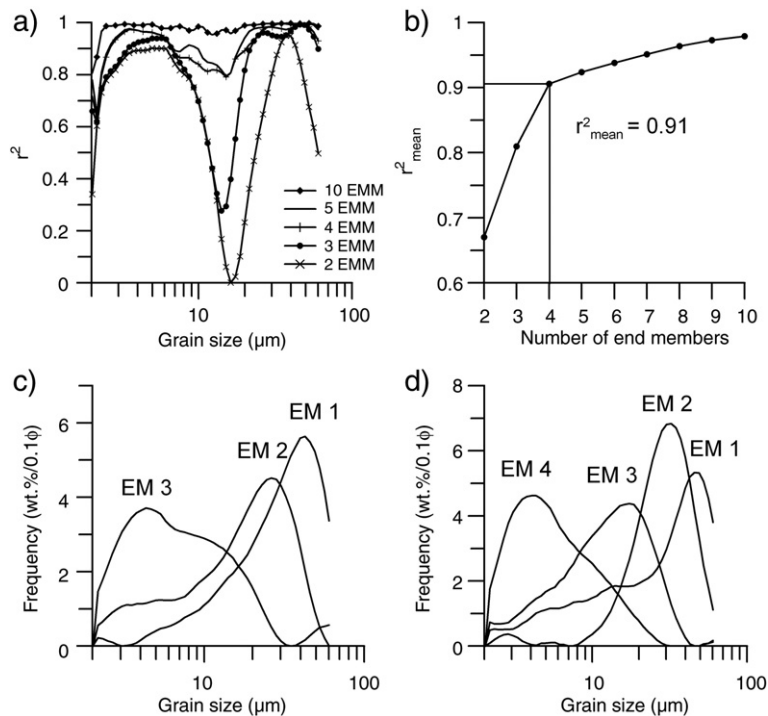


Fig. 8. Results from end-member modelling of the analysed grain-size distributions of the hemipelagic carbonate-free silt fractions of cores GeoB 8502–2, GeoB 8507–3 and GeoB 8509–2. a) The coefficients of determination (r^2) are plotted for each size class of the different end-member solutions. b) Mean coefficient of determination (r^2_{mean}) for each end-member model from two to ten end members. c) End-member grain-size distributions for the three-end-member model. d) Modelled grain-size distributions for the four-end-member solution.

spectrum. A comparison of the end-member grain-size distributions of the two models indicates that the finest end member of the three-end-member model is split in two discrete subpopulations (EM 3 and EM 4; Fig. 8d). In addition to the better statistical fit, the downcore relative proportions of the four end members reveal more details in terms of terrigenous transport processes and environmental changes in the African hinterland. The grain-size distributions of the four-end-member model (Fig. 8d) are unimodal, well sorted, and are widely distributed over the measured size spectrum. The coarsest end member (EM 4; Fig. 8d) shows a modal grain size of $\sim 45 \mu\text{m}$, whereas EM 3 and EM 2 have modes around 32 and 17 μm , respectively. Since grain-size distributions have been determined for the undisturbed sediments only, turbidity currents are excluded here as transport process relevant for one of the coarse end members. Present-day aeolian dust, which was collected along a transect of the north-west African coast between $\sim 33^\circ\text{N}$ and $\sim 12^\circ\text{S}$, was shown to vary between 8 and 48 μm and indicates that aeolian dust supply covers a wide spectrum of grain sizes due to different regional settings and sources (Stuut et al., 2005). In accordance to this and to results of previous

studies of seabed samples along this margin and downcore marine records off Morocco (Holz et al., 2004, in review), the three coarsest end members (EM 1 to EM 3) are interpreted to represent different populations or sources of aeolian dust supply. With a modal grain size of about 4 μm the finest calculated end-member distribution (EM 4) is much finer than the previous and may result from other processes such as fluvial supply (e.g., Koopmann, 1981; Holz et al., 2004) or long travelling dust transport. Studies with large source to sink distances have shown that wind-blown dust can be very fine in size (Rea, 1994; Rea and Hovan, 1995). Another possible explanation for these fine sediments is sediment redistribution by bottom currents.

Relative contributions of the end-member grain-size distributions downcore can be used as proxies for palaeoclimate reconstructions on the adjacent continent. During late Pleistocene times dominantly coarse-grained particles were deposited off north-west Africa (Fig. 9). EM 3 and EM 2 are relatively consistent throughout the Pleistocene, whereas the coarser end-member grain-size distribution represents the dominant size fraction and may be related to a different source. Relative proportions of EM 1 increase significantly during several intervals

throughout the late Pleistocene. These contributions of the three coarsest end-member grain-size distributions decrease with the onset of the Holocene. In contrast, the finest end member is significantly represented for the first time at the beginning of the Holocene and reaches its maximal contribution during the mid Holocene. In the following time period, relative proportions of EM 4 decrease to the present time.

5. Sedimentation of Cap Timiris Canyon — indications for fluvial runoff during the Holocene?

The investigated hemipelagic sediments display an overall similar sedimentation pattern for the three Cap Timiris Canyon locations, which also includes the intra-canyon site GeoB 8509–2 and thus, are all used here for the following palaeoclimate reconstruction.

5.1. Proximal and distal sedimentation

Comparing the proximal and distal data sets, slightly higher sand and carbonate contents are observed for

the distal levee site of Cap Timiris Canyon. Furthermore, this site is characterised by the lowest terrigenous silt content of all considered records, which illustrates the offshore decreasing impact of the African continent on the depositional system of Cap Timiris Canyon. The correspondence of the sand and carbonate records indicate higher planktonic foraminifer concentrations. Furthermore, it provides evidence for a predominantly pelagic influence and less dilution by terrigenous material at site GeoB 8502–2 on the lower levee of Cap Timiris Canyon. In addition, modal grain sizes of the terrigenous silt fraction document a downwind fining in particle size and a downwind decrease in transport capacity of the winds. For the distal levee site the shift in sedimentation to a more pronounced pelagic character is accentuated by bimodal grain-size distributions of the carbonate silt fraction. Particles show modal grain-sizes around 4 to 5 μm and 22 μm , presumably representing coccoliths and fragments of foraminifers (Robinson and McCave, 1994; McCave et al., 1995; Frenz et al., 2005), respectively.

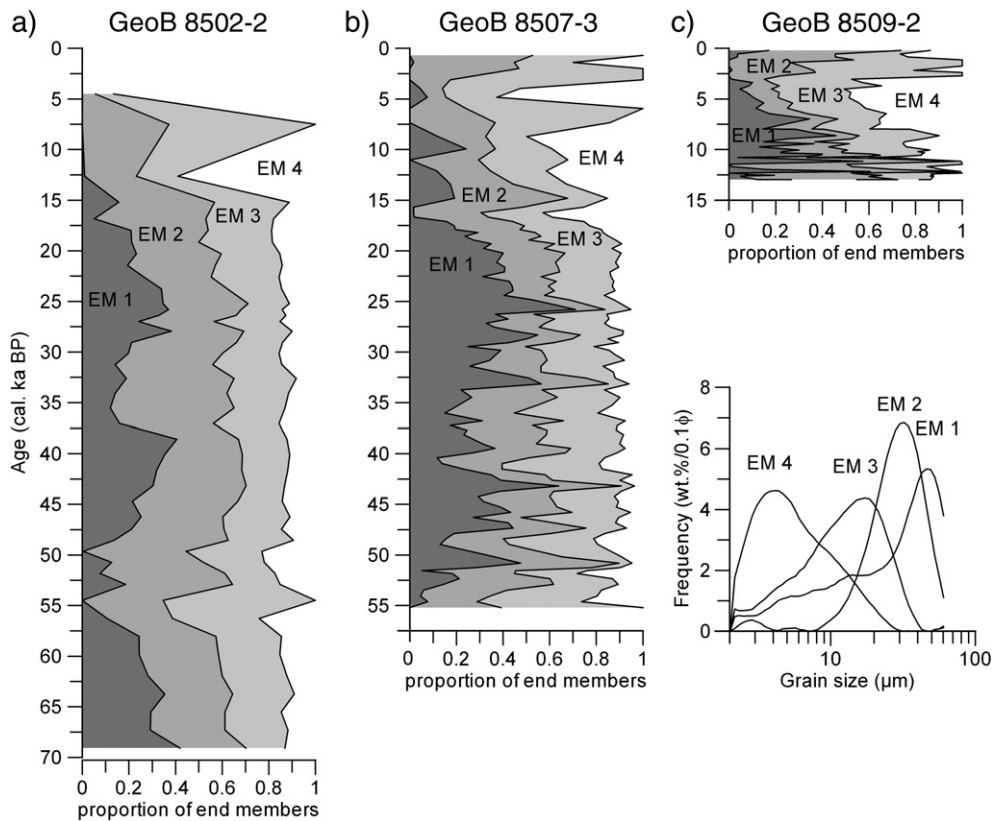


Fig. 9. Relative proportions of modelled end-member grain-size distributions for a) the distal levee site GeoB 8502–2, b) the proximal levee record GeoB 8507–3 and c) the intra-canyon core GeoB 8509–2 of Cap Timiris Canyon since late Pleistocene times. Note that the age model of sediment core GeoB 8509–2 is based on radiocarbon dates. According to the core-to-core correlation it would date back to ~15 ka (Wien et al., 2006, see also 3.1 this study).

5.2. Sedimentation and climate change

During the Pleistocene, hemipelagic sedimentation around Cap Timiris Canyon varies spatially depending on the distance to the African continent. Throughout the Pleistocene, sedimentation is characterised by fine-grained material ($<63\ \mu\text{m}$), predominantly by sediments of the coarse silt fraction. Although main components are of biogenic origin, a pronounced terrigenous signal is recognised in the silt fraction offshore Cap Timiris. This indicates an increased availability of terrigenous sediments, which might have easily been transported across the shelf break during Pleistocene sea-level lowstands. Modelled end members from grain-size analyses of Cap Timiris Canyon sediments are similar to those revealed from seabed samples along the north-west African continental margin (Holz et al., 2004). Furthermore, the trends found in the end-member distributions off Mauritania are almost identical with those depicted for a last deglacial to Holocene marine downcore record offshore Morocco (Holz et al., in review). In these studies, modelled end members are compared to present-day aeolian dust fallout along the north-west African continental margin (Stuut et al., 2005) and are attributed to different transport processes (e.g., aeolian dust and fluvial supply) that reflect climatic conditions of the adjacent continent. Accordingly, the coarsest end members of this study, EM 1, EM 2 and EM 3, are attributed to different size fractions of aeolian dust deposition. However, it should be borne in mind that an interaction during transport, deposition and redistribution may also result from other processes such as winnowing by bottom currents. Winnowing can principally affect sediment coarsening because fine particles are sorted out. Poorly developed levees may support sediment sorting by bottom currents, although bottom current velocities in this region are at least nowadays assumed to be fairly weak ($<5\ \text{cm s}^{-1}$) but may increase to $20\ \text{cm s}^{-1}$ in areas where currents are focussed by morphology (Lonsdale, 1982; Sarnthein et al., 1982). Moreover, assuming bottom current winnowing to be active, it would be expected that not only the terrigenous fraction in the sediment is affected by sediment redistribution but also the carbonate fraction (cp. Fig. 5). However, since the carbonate silt shows bimodal distributions with modes in the coarse and in the fine silt fraction, we stay with the interpretation of a primarily aeolian dust signal. Variations in wind intensities affect favoured particle sizes of wind-blown sediments. Many dust-plume events of different strengths occur throughout a year. As each sample taken from the sedimentary record represents many years of accumulation, it will always contain a mixture of

multiple dust events consisting of coarse- and fine-grained particles. EM 4 with a modal grain size of about $4\ \mu\text{m}$ is significantly finer and illustrates an almost identical result as in previous models of terrigenous sediment compositions offshore north-west Africa (Holz et al., 2004, in review). Therein it was interpreted to originate predominantly from fluvial discharge, although a certain proportion may be attributed to very fine wind-blown dust that was transported over long distances.

Based on this interpretation aeolian deposition dominates the terrigenous sediment transport off north-west Africa throughout the Pleistocene marine isotope stages 4 to 2. Depending on the prevailing wind strength, the aeolian input varies between coarse- and fine-grained dust fallout represented by the three coarsest end members, whereas the relative proportion of EM 4 is negligible during this time (Fig. 9). These findings of enhanced aeolian sediment supply off Cap Timiris are in agreement with the association of an arid glacial climate and a general sediment mobilisation rather than stabilisation in northern Africa (e.g., Sarnthein and Diester-Haass, 1977; Swezey, 2001). Onshore and marine proxy studies have shown that arid conditions prevailed in north-west Africa during the late Pleistocene (e.g., Koopmann, 1981; Sarnthein et al., 1982; Van Andel and Tzedakis, 1996; deMenocal et al., 2000). During this time, western Mauritania was dominated by extensive sand seas and linear sand dunes, which extended onto the continental shelf during periods of low sea level (Sarnthein and Diester-Haass, 1977; Lancaster et al., 2002). The arid climate and sand dunes offered optimal conditions for terrigenous sediment transport offshore in terms of aeolian dust input. Fluvial drainage to the Atlantic Ocean offshore Mauritania was less important during the isotopic stages 4, 3, and 2, although the origin of Cap Timiris Canyon is assumed to be linked to an ancient river system that breached the shelf during a Plio/Pleistocene sea-level lowstand (Antobreh and Krastel, 2006). This is furthermore consistent with findings of a potential, topography-deduced major river system, named Tamanrasset, which however is non-discharging under recent climate conditions (Vörösmarty et al., 2000). Presently, the Senegal River is the northernmost active drainage system of West Africa. Between the Senegal River in the south and about $29\text{--}30^\circ$ northern latitude, fluvial discharge is of subordinate importance along the north-west African continental margin (Holz et al., 2004). However, according to previous studies (Michel, 1980; cited in Koopmann, 1981), the Senegal River is also not supposed to have reached the Atlantic Ocean during the last glacial. In these studies, age estimates for a first breakthrough across the coastal and shelf dune fields are centred between 13 and 12 ka.

Around this time, a significant change in the previously homogenous sedimentation pattern of Cap Timiris Canyon can be observed from the studied cores. During the Pleistocene, sedimentation rates for the distal (GeoB 8502–2) and proximal (GeoB 8507–3) levee sites were determined to be on average 6 cm/ka and 19 cm/ka, respectively, whereas average Holocene sedimentation rates are reduced by approximately one half to 3.5 cm/ka and 10 cm/ka for the two mentioned levee sites. The silt contents are decreased in favour of sand and clay contents and the terrigenous influence is reduced while carbonate sedimentation is enhanced with the onset of the Holocene humid period (Fig. 4). The shift to finer particle sizes for the terrigenous silt fraction at all three sites nicely portrays the change in north-west African climate, which is also visible from the modelled end-member grain-size distributions. The interpretation follows the previously established pattern of late Pleistocene arid conditions, a humid early to mid Holocene, and a return to more arid climate conditions in the late Holocene (e.g., Sarnthein et al., 1981; Lézine and Casanova, 1989; deMenocal et al., 2000). During the onset of the Holocene, transport of the coarsest aeolian dust particles (EM 1), which occurred during glacial times, seems to be less important in favour of aeolian dust particles around 32 and 17 μm . During Holocene times, the finest end member (EM 4) is significantly represented for the first time, although its relative proportions are decreasing from maximum values in the middle Holocene to minimum values in the late Holocene (Fig. 9). The assumption that it characterises predominantly fluvial supply to the Atlantic Ocean is consistent with findings of a general aeolian sediment stabilisation from early to mid Holocene (Swezey, 2001). As mentioned above, the Senegal River did not reach the Atlantic Ocean during the last glacial period until about 13 or 12 ka ago (Michel, 1980; cited in Koopmann, 1981). Numerous onshore records indicate that humid conditions existed in the Saharan region during the early and mid Holocene (summarised in Gasse, 2000; Kuper and Kröpelin, 2006). Rising lake levels are reported from central Africa and particularly from the Chad basin during this time (Maley, 1977). For east Africa the Holocene African Humid Period was described by Ritchie et al. (1985) and Roberts (1998) between 9 and 6 ka. Humid conditions and enhanced fluvial runoff are also reported from the Mediterranean region during \sim 9.25 and 7.25 ka (Arz et al., 2003), while the onset of humid conditions in tropical west Africa, is proposed at 9–6.3 ka and 4–2.5 ka (Lézine and Casanova, 1989). Deduced from an abrupt change in terrigenous sediment input off Cape Blanc, deMenocal et al. (2000) proposed the onset of humid conditions in this area around 14.5 ka. The freshwater

discharge of the Niger River to the ocean increased from about 13.6 ka and became very large in the Holocene between 11.5 and 4 ka (Pastouret et al., 1978). Along the continental slope between the Cape Verde Islands in the south, and southern Mauritania in the north, an enhanced supply of fine-grained material in the terrigenous fraction was related to northward winnowed fluvial runoff from the Senegal, Gambia, and Saloum Rivers during the Holocene climatic optimum and for the present day (Koopmann, 1981; Sarnthein et al., 1982). Furthermore, Lézine (1987; cited in Lézine and Casanova, 1989) recorded evidence that surficial runoff in the littoral interdunes of the southern Sahara occurred as early as 12 ka. To summarise, numerous studies indicate an onset of humid conditions and suggest a fluvial influence around the beginning of the Holocene period. However, indications for fluvial supply and thus for a former fluvial point source in northern Mauritania discharging to a canyon, which itself being only recently discovered (Kraestel et al., 2004), are missing in previous data sets. Cap Timiris Canyon may have represented the main drainage system of Mauritania during early and mid Holocene times. If so, it can be assumed that fluvial mud is funnelled in the tributary system on the Mauritanian shelf before being transported downslope within the system.

In contrast, the late Holocene situation is characterised by progressively increasing aridity in the Mauritanian hinterland, with a more widespread aeolian sediment mobilisation and a return to dune activity that persists until the present day, although there are indications for brief phases of fluvial–lacustrine deposition and aeolian sediment stabilisation (Swezey, 2001; Lancaster et al., 2002). This development is also in agreement with the end-member grain-size distributions. The finest end member (EM 4) is continuously decreasing, which indicates the return to more arid conditions with the lowest proportions for the present day. This perfectly fits with the recent situation of a starved river system in Mauritania, the Tamanrasset River (Vörösmarty et al., 2000), while further south the Senegal River is still draining to the Atlantic Ocean.

6. Conclusions

This study shows that hemipelagic sediments, which are intercalated by turbidite deposits, can be used for palaeoclimatic reconstructions by differentiating carefully between hemipelagic and gravity-driven sedimentary processes. Sediments of the investigated sites illustrate (1) that sedimentation is affected by different processes on the proximal and distal levee as well as in the canyon itself and (2) that glacial–interglacial climate

changes characterise the sedimentation pattern around Cap Timiris Canyon. Aeolian deposition dominated during the arid glacial period of isotopic stages 4, 3, and 2. This pattern changed with the onset of the Holocene humid period. Fluvial discharge into the Atlantic Ocean through the Cap Timiris Canyon system may have been re-activated in early and mid Holocene times. Further on during the late Holocene, progressive desertification led to a starvation of the terrestrial part of Cap Timiris Canyon in Mauritania, which is contrary to the situation of the Senegal River further southwards. Thus, Cap Timiris Canyon is one of very few prominent examples of a huge submarine meandering channel system that does not have a recent obvious or even active connection to a sub-aerial river system in the hinterland and which might be the reason that it was investigated only recently.

Acknowledgements

The captain, crew, and shipboard participants of cruise M58/1 are thanked for their assistance during retrieval of the sediment cores. The authors greatly acknowledge Maarten Prins for the help with the end-member calculations and Gert Jan Weltje for providing the end-member algorithm. We are grateful to Janine Bardenhagen for providing carbonate data of GeoB 8509–2 (unpublished thesis). B. Kockisch, H. Heilmann and U. Proske are thanked for technical assistance in the laboratory. The manuscript benefits from reviews by two anonymous referees. This work was funded by the Deutsche Forschungsgemeinschaft as part of the DFG-Research Center Ocean Margins of the University of Bremen. It is contribution RCOM0466.

References

- Antobreh, A.A., Krastel, S., 2006. Morphology, seismic characteristics and development of Cap Timiris Canyon, offshore Mauritania: a newly discovered canyon preserved-off a major arid climatic region. *Mar. Pet. Geol.* 23 (1), 37–59.
- Arz, H., Lamy, F., Pätzold, J., Müller, P.J., Prins, M.A., 2003. Mediterranean moisture source for an early-Holocene humid period in the northern Red Sea. *Science* 300 (5616), 118–122.
- Bein, A., Fütterer, D., 1977. Texture and composition of continental shelf to rise sediments off the northwestern coast of Africa: an indicator for downslope transportation. *Meteor. Forschungsber.* 27 (C), 46–74.
- deMenocal, P., Ortiz, J., Guilderson, T., Adkins, J., Sarnthein, M., Baker, L., Yarusinsky, M., 2000. Abrupt onset and termination of the African Humid Period: rapid climate responses to gradual insolation forcing. *Quat. Sci. Rev.* 19 (1–5), 347–361.
- Diester-Haass, L., 1981. Factors contributing to Late Glacial and Holocene sedimentation on the continental shelf and slope off NW Africa, Banc d'Arguin, 19°N. *Meteor. Forschungsber.* 35 (C), 1–22.
- Dupont, L.M., Beug, H.-J., Stalling, H., Tiedemann, R., 1989. First Palynological results from Site 658 at 21°N off Northwest Africa: pollen as climate indicators. In: Ruddiman, W., Sarnthein, M., et al. (Eds.), *Proceedings of the Ocean Drilling Program, Scientific Results*, College Station, Texas, pp. 93–111.
- Faugères, J.C., Legigan, P., Maillet, N., Sarnthein, M., Stein, R., 1989. Characteristics and distribution of Neogene turbidites at Site 657 (Leg 108, Cap Blanc continental rise, Northwest Africa): variations in turbidite source and continental climate. In: Ruddiman, W., Sarnthein, M., et al. (Eds.), *Proceedings of the Ocean Drilling Program, Scientific Results*, College Station, Texas, pp. 329–348.
- Frenz, M., Höppner, R., Stuut, J.-B.W., Wagner, T., Henrich, R., 2003. Surface sediment bulk geochemistry and grain-size composition related to the oceanic circulation along the South American continental margin in the Southwest Atlantic. In: Mulitza, S., Ratmeyer, V., Wefer, G. (Eds.), *The South Atlantic in the late Quaternary: Reconstruction of Material Budget and Current Systems*. Springer, Berlin, pp. 347–373.
- Frenz, M., Baumann, K.-H., Böckel, B., Höppner, R., Henrich, R., 2005. Quantification of foraminifer and coccolith carbonate in South Atlantic surface sediments by means of carbonate grain-size distributions. *J. Sediment. Res.* 75 (3), 464–475.
- Fütterer, D.K., 1983. The modern upwelling record off Northwest Africa. In: Thiede, J., Suess, E. (Eds.), *Coastal Upwelling: Its Sediment Record, Part B. Sedimentary Records of Ancient Coastal Upwelling*. Plenum Press, London, pp. 105–121.
- Gasse, F., 2000. Hydrological changes in the African tropics since the Last Glacial Maximum. *Quat. Sci. Rev.* 19 (1–5), 189–211.
- Gasse, F., Van Campo, E., 1994. Abrupt post-glacial climate events in West Asia and North Africa monsoon domains. *Earth Planet. Sci. Lett.* 126 (4), 435–456.
- GEBCO, 2003. *General Bathymetric Chart of the Oceans*. IHO-UNESCO.
- Hagen, E., 2001. Northwest African upwelling scenario. *Oceanol. Acta* 24 (Supplement), 113–128.
- Hillier, S., 1995. Erosion, Sedimentation, and Sedimentary Origin of Clays. In: Velde, B. (Ed.), *Origin and Mineralogy of Clays — Clays and the Environment*. Springer Verlag, Berlin, pp. 162–219.
- Holz, C., Stuut, J.-B.W., Henrich, R., 2004. Terrigenous sedimentation processes along the continental margin off NW-Africa: implications from grain-size analysis of seabed sediments. *Sedimentology* 51 (5), 1145–1154.
- Holz, C., Stuut, J.-B.W., Henrich, R., Meggers, H., in review. Variability in terrigenous sedimentation processes off Northwest Africa and its relation to climate changes: inferences from grain-size distributions of a Holocene marine sediment record. *Sediment. Geol.*
- Hughen, K.A., Baillie, M.G.L., Bard, E., Beck, J.W., Bertrand, C.J.H., Blackwell, P.G., Buck, C.E., Burr, G.S., Cutler, K.B., Damon, P.E., Edwards, R.L., Fairbanks, R.G., Friedrich, M., Guilderson, T.P., Kromer, B., McCormac, G., Manning, S., Ramsey, C.B., Reimer, P.J., Reimer, R.W., Remmele, S., Southon, J.R., Stuiver, M., Talamo, S., Taylor, F.W., van der Plicht, J., Weyhenmeyer, C.E., 2004. Marine04 Marine Radiocarbon Age Calibration, 0–26 Cal Kyr BP. *Radiocarbon* 46 (3), 1059–1086.
- Jakobi, R.D., Hayes, D.E., 1982. Bathymetry, microphysography and reflectivity characteristics of the West African Margin between Sierra Leone and Mauritania. In: Von Rad, U., Hinz, K., Sarnthein, M., Seibold, E. (Eds.), *Geology of the Northwest African continental margin*. Springer-Verlag, Heidelberg, pp. 182–210.

- Koopmann, B., 1981. Sedimentation von Saharastaub im subtropischen Nordatlantik während der letzten 25.000 Jahre. *Meteor Forschungsergeb.* 35, 23–59.
- Koukoku, G.L., Barusseau, J.P., 1988. Terrigenous sedimentation of the upper Quaternary in the Cayar deep-sea fan (Senegal–Gambia). *Oceanol. Acta* 11 (4), 359–368.
- Krastel, S., Hanebuth, T.J.J., Antobreh, A.A., Henrich, R., Holz, C., Kölling, M., Schulz, H.D., Wien, K., Wynn, R.B., 2004. Cap Timiris Canyon: A newly discovered channel-system off Mauritania. *Eos, Trans. - Am. Geophys. Union* 85 (42), 417–432.
- Krastel, S., Wynn, R.B., Hanebuth, T.J.J., Henrich, R., Holz, C., Meggers, H., Kuhlmann, H., Georgiopoulou, A., Schulz, H.D., 2006. Mapping of seabed morphology and shallow sediment structure of the Mauritania continental margin, North Africa: some implications on the geohazard potential. *Nor. J. Geol.* 86, 163–176.
- Kuper, R., Kröpelin, S., 2006. Climate-controlled Holocene occupation in the Sahara: Motor of Africa's evolution. *Science* 313, 803–807.
- Lancaster, N., Kocurek, G., Singhvi, A., Pandey, V., Deynoux, M., Ghienne, J.-F., Lô, K., 2002. Late Pleistocene and Holocene dune activity and wind regimes in the western Sahara Desert of Mauritania. *Geology* 30 (11), 991–994.
- Lézine, A.-M., 1987. Paléoenvironnements végétaux d'Afrique nord-tropicale depuis 12000 B.P. Unpublished Thesis, University of Aix-Marseille, 180 pp.
- Lézine, A.-M., Casanova, J., 1989. Pollen and hydrological evidence for the interpretation of past climates in tropical west Africa during the Holocene. *Quat. Sci. Rev.* 8, 45–55.
- Lonsdale, P., 1982. Sediment drift of the Northeast Atlantic and their relationship to the observed abyssal currents. *Bull. Inst. Geol. Bassin Aquitaine, Bordeaux*, 141–150.
- Maley, J., 1977. Palaeoclimates of Central Sahara during the early Holocene. *Nature* 269, 573–577.
- Matthewson, A.P., Shimmield, G.B., Kroon, D., Fallick, A.E., 1995. A 300 kyr high-resolution aridity record of the North African continent. *Paleoceanography* 10 (3), 677–692.
- McCave, I.N., Manighetti, B., Robinson, S.G., 1995. Sortable silt and fine sediment size/composition slicing: parameters for palaeocurrent speed and palaeoceanography. *Paleoceanography* 10 (3), 593–610.
- McMaster, R.L., Lachance, T.P., 1969. Northwestern African continental shelf sediments. *Mar. Geol.* 7, 57–67.
- Michel, P., 1980. The Southwestern Sahara margin. *Paleoecol. Africa* 12, 297–306.
- Mienert, J., Weaver, P.E.E. (Eds.), 2003. European margin sediment dynamics: side-scan sonar and seismic images. Springer-Verlag, Berlin, 309 pp.
- Pastouret, L., Chamley, H., Delibrias, G., Duplessy, J.C., Thiede, J., 1978. Late Quaternary climatic changes in Western tropical Africa deduced from deep-sea sedimentation off the Niger delta. *Oceanol. Acta* 1, 217–232.
- Prins, M.A., Weltje, G.J., 1999. End-member modeling of siliciclastic grain-size distributions: the late Quaternary record of eolian and fluvial sediment supply to the Arabian Sea and its paleoclimatic significance. In: Harbaugh, J.W., Watney, W.L., Rankey, E.C., Slingerland, R., Goldstein, R.H., Franseen, E.K. (Eds.), *Numerical Experiments in Stratigraphy; Recent Advances in Stratigraphic and Sedimentologic Computer Simulations*, pp. 91–111.
- Ratmeyer, V., Fischer, G., Wefer, G., 1999. Lithogenic particle fluxes and grain size distributions in the deep ocean off northwest Africa: implications for seasonal changes of aeolian dust input and downward transport. *Deep-Sea Res. (I)* 46, 1289–1337.
- Rea, D.K., 1994. The paleoclimatic record provided by eolian deposition in the deep sea: the geologic history of wind. *Rev. Geophys.* 32 (2), 159–195.
- Rea, D.K., Hovan, S.A., 1995. Grain size distribution and depositional processes of the mineral component of abyssal sediments: lessons from the North Pacific. *Paleoceanography* 10 (2), 251–258.
- Ritchie, J.C., Eyles, C.H., Haynes, C.V., 1985. Sediment and pollen evidence for an early to mid-Holocene humid period in the eastern Sahara. *Nature* 330, 645–647.
- Roberts, N., 1998. *The Holocene*. Blackwell, Oxford, 316 pp.
- Robinson, S.G., McCave, N.I., 1994. Orbital forcing of bottom-current enhanced sedimentation on Feni Drift, NE Atlantic, during the mid-Pleistocene. *Paleoceanography* 9 (6), 943–972.
- Rust, U., Wienecke, F., 1973. Bathymetrische und geomorphologische Bearbeitung von submarinen "Einschnitten" im Seegebiet vor Westafrika. Ein Method. Vers. Münch. Geogr. Abh. 9, 53–66.
- Sarnthein, M., 1978. Sand deserts during glacial maximum and climatic optimum. *Nature* 272, 43–46.
- Sarnthein, M., Diester-Haass, L., 1977. Eolian-sand turbidites. *J. Sediment. Petrol.* 47, 868–890.
- Sarnthein, M., Tetzlaff, G., Koopmann, B., Wolter, K., Pflaumann, U., 1981. Glacial and interglacial wind regimes over the eastern subtropical Atlantic and North-West Africa. *Nature* 293, 193–296.
- Sarnthein, M., Thiede, J., Pflaumann, U., Erlenkeuser, H., Fütterer, D., Koopmann, B., Lange, H., Seibold, E., 1982. Atmospheric and Oceanic Circulation Patterns off Northwest Africa During the Past 25 Million Years. In: von Rad, U., Hinz, K., Sarnthein, M., Seibold, E. (Eds.), *Geology of the Northwest African Continental Margin*. Springer-Verlag, Heidelberg, pp. 545–604.
- Schulz, H.D., cruise participants, 2003. Report and Preliminary Results of METEOR Cruise M58/1, Dakar — Las Palmas, 15.04–12.05.2003. Berichte aus dem Fachbereich Geowissenschaften, Universität Bremen, No. 215 Bremen, 186 pp.
- Seibold, E., Diester-Haass, L., Fütterer, D., Hartmann, M., Kögler, F.C., Lange, H., Müller, P.J., Pflaumann, U., Schrader, H.J., Suess, E., 1976. Late Quaternary Sedimentation off the Western Sahara. In: De Almeida, F.F.M. (Ed.), *Continental Margins of Atlantic Type*. An. Acad. bras. Cienc., pp. 287–296.
- Shaffer, G., 1976. A mesoscale study of coastal upwelling variability off NW Africa. *Meteor Forschungsergeb.* 17 (A), 21–72.
- Stabell, B., 1989. Initial diatom record of sites 657 and 658: on the history of upwelling and continental aridity. In: Ruddiman, W., Sarnthein, M., et al. (Eds.), *Proceedings of the Ocean Drilling Program, Scientific Results, College Station, Texas*, pp. 149–156.
- Street-Perrott, F.A., Perrott, R.A., 1990. Abrupt climate fluctuations in the tropics: the influence of Atlantic Ocean circulation. *Nature* 343, 607–612.
- Stuiver, M., Reimer, P.J., 1993. Extended 14C database and revised CALIB radiocarbon calibration program. 4.4.2. *Radiocarbon* 35, 215–230.
- Stuut, J.B.W., Lamy, F., 2004. Climate variability at the southern boundaries of the Namib (southwestern Africa) and Atacama (northern Chile) coastal deserts during the last 120,000 yr. *Quat. Res.* 62, 301–309.
- Stuut, J.-B.W., Prins, M.A., Schneider, R.R., Weltje, G.J., Jansen, J.H.F., Postma, G., 2002. A 300-kyr record of aridity and wind strength in southwest Africa: inferences from grain-size distributions of sediments on Walvis Ridge, SE Atlantic. *Mar. Geol.* 180, 221–233.
- Stuut, J.-B.W., Zabel, M., Ratmeyer, V., Helmke, P., Schefuß, E., Lavik, G., Schneider, R.R., 2005. Provenance of present-day eolian dust collected off NW Africa. *J. Geophys. Res.* 110. doi:10.1029/2004JD005161.

- Summerhayes, C.P., 1983. Sedimentation of organic matter in upwelling regimes. In: Thiede, J., Suess, E. (Eds.), *Coastal Upwelling: Its Sediment Record*, Part B. Plenum Press, London, pp. 29–72.
- Swezey, C., 2001. Eolian sediment responses to late Quaternary climate changes: temporal and spatial patterns in the Sahara. *Palaeogeogr. Palaeoclimatol. Palaeoecol.* 167 (1–2), 119–155.
- Tiedemann, R., Sarnthein, M., Stein, R., 1989. Climatic Changes In The Western Sahara: Aeolo-Marine Sediment Record of The Last 8 Million Years (Sites 657–661). In: Ruddiman, W., Sarnthein, M., et al. (Eds.), *Proceedings of the Ocean Drilling Program, Scientific Results*, College Station, Texas, pp. 241–277.
- Van Andel, T.H., Tzedakis, P.C., 1996. Palaeolithic landscapes of Europe and environs, 150,000–25,000 years ago: an overview. *Quat. Sci. Rev.* 15 (5–6), 481–500.
- Van Camp, L., Nykjaer, L., Mittelstaedt, E., Schlittenhardt, P., 1991. Upwelling and boundary circulation off Northwest Africa as depicted by infrared and visible satellite observations. *Prog. Oceanogr.* 26 (4), 357–402.
- Vörösmarty, C.J., Fekete, B.M., Meybeck, M., Lammers, R.B., 2000. Global system of rivers: its role in organizing continental land mass and defining land-to-ocean linkages. *Glob. Biogeochem. Cycles* 14 (2), 599–621.
- Weaver, P.P.E., Wynn, R.B., Kenyon, N.H., Evans, J., 2000. Continental margin sedimentation, with special reference to the north-east Atlantic margin. *Sedimentology* 47 (Suppl. 1), 239–256.
- Weltje, G.J., 1994. Provenance and dispersal of sand-sized sediments: reconstruction of dispersal patterns and sources of sand-sized sediments by means of inverse modelling techniques. Ph.D. Thesis, *Geologica Ultraiectina*, 208 pp.
- Weltje, G.J., 1997. End-member modeling of compositional data: numerical–statistical algorithms for solving the explicit mixing problem. *J. Math. Geol.* 29, 503–549.
- Weltje, G.J., Prins, M.A., 2003. Muddled or mixed? Inferring palaeoclimate from size distributions of deep-sea clastics. *Sediment. Geol.* 162 (1–2), 39–62.
- Wien, K., Holz, C., Kölling, M., Schulz, H.D., 2006. Age models for pelagites and turbidites from the Cap Timiris Canyon off Mauritania. *Mar. Pet. Geol.* 23 (3), 337–352.
- Wynn, R.B., Masson, D.G., Stow, D.A.V., Weaver, P.P.E., 2000. The Northwest African slope apron: a modern analogue for deep-water systems with complex seafloor topography. *Mar. Pet. Geol.* 17 (2), 253–265.